International Journal of Materials Science
ISSN 0973-4589 Volume 12, Number 4 (2017), pp. 561-570

http://www.ripublication.com

Influence of Rare-Earth concentration on the crystallization process and application of Kissinger, Augis-Bennet and Matusita-Sakka equations to kinetics analysis of amorphous $Fe_{78}Tm_2B_{20}$ and $Fe_{76}Tm_4B_{20}$ alloys

M.D.V. Srilalitha[1*] and B. Bhanu Prasad[2]

[1]Pursuing Ph.D at Rayalaseema University (PP PHY 0134) , Kurnool, India.
[2]Department of Sciences & Humanities, M.V.S.R. Engineering College, Nadergul, Hyderabad, India.
**Corresponding author*

Abstract

The crystallization behavior of amorphous $Fe_{78}Tm_2B_{20}$ and $Fe_{76}Tm_4B_{20}$ alloys were carefully investigated in response to heat treatment using a combination of differential scanning calorimetry (DSC) and X-ray diffraction (XRD). The crystallization process of amorphous $Fe_{76}Tm_4B_{20}$ alloy strongly differs from that of amorphous $Fe_{78}Tm_2B_{20}$ alloy. The grain size of the samples were calculated from annealing studies using room temperature XRD. The grain size of the samples increases with increase in annealing temperature and with the increase in concentration of Tm in Fe-B. XRD results showed the presence of α – Fe. Kinetic investigation of crystallization on amorphous $Fe_{78}Tm_2B_{20}$ and $Fe_{76}Tm_4B_{20}$ alloys has been done using DSC. The activation energy of crystallization(E_a) and Frequency factor(k_0) have been calculated in the frame of three models namely Kissinger, Augis-Bennet and Matusita-Sakka. The average activation energy for primary crystallization of amorphous $Fe_{78}Tm_2B_{20}$ and $Fe_{76}Tm_4B_{20}$ alloys using the above three methods is found to be 385.30kJouls/mole and 430.86 kJouls/mole, respectively. The frequency factor of amorphous $Fe_{78}Tm_2B_{20}$ and $Fe_{76}Tm_4B_{20}$ alloys using Kissinger method is found to be $2.47x10^{21}$ $(sec)^{-1}$ and $5.39x10^{17}$ $(sec)^{-1}$, respectively. The frequency factor of amorphous $Fe_{78}Tm_2B_{20}$ and $Fe_{76}Tm_4B_{20}$ alloys using

Augis-Bennet's method is found to be 8.6 $7x10^{22}$ $(sec)^{-1}$ and $2.51x10^{19}$ $(sec)^{-1}$, respectively.

Keywords: differential scanning calorimetry, activation energy, crystallization temperature, phase transformation, room temperature

INTRODUCTION

In the last two decades, quite numerous studies were dedicated to ternary amorphous systems containing Transition Metal (TM), Rare-Earth (RE) and Metalloid Elements (ME), particularly with compositions such as

$(TM)_{80-x}$ $(RE)_x$ $(ME)_{20}$ [1]. The theory of crystallization in amorphous materials can be explained by considering the structure and the kinetics of the crystallization. Therefore, the investigation of crystallization kinetics is important since it quantifies the effect of the nucleation and growth rate of the resulting crystallites [2]. Crystallization kinetics of amorphous materials was investigated by explaining the crystallization mechanism and the crystallization activation energy in terms of non isothermal methods with different approaches. Differential thermal analysis (DTA) techniques used in crystallization kinetic studies were presented and a correlation between kinetic and structural investigations was made to determine the crystallization mechanism [3,4]. In this paper, we present the i*nfluence of Rare-Earth concentration on the crystallization process and* the a*pplication of* Kissinger, Augis-Bennet and Matusita-Sakka *equations to kinetics analysis of amorphous* $Fe_{78}Tm_2B_{20}$ and $Fe_{76}Tm_4B_{20}$ alloys using DSC and XRD.

EXPERIMENTAL

Specimens of amorphous $Fe_{78}Tm_2B_{20}$ and $Fe_{76}Tm_4B_{20}$ ribbons prepared by single roller melt spinning technique under inert atmosphere were procured from our other researchers. The alloy ribbons were about 1 mm wide and about 30 μm thick. The amorphous nature of ribbons was confirmed by X-ray diffraction (XRD).The as-quenched samples of $Fe_{78}Tm_2B_{20}$ and $Fe_{76}Tm_4B_{20}$ ribbons were heated using differential scanning calorimetry(DSC) at four linear heating rates (5, 10, 15 and 20 Kelvin/min) from room temperature to 1200 K. The DSC scans were recorded by a thermal analyzer interfaced to a computer. The structural characterizastion was carried out by x-ray diffraction. The samples of amorphous alloy $Fe_{78}Tm_2B_{20}$ and $Fe_{76}Tm_4B_{20}$ were annealed at different temperatures say at 500^{o}C, 600^{o}C and 700^{o}C for one hour. The x-ray diffraction measurements were performed on SHIMADZU XRD-7000 X-RAY DIFFRACTOMETER using Cu - Kα radiation over a 2theta angle range of 10-80 degrees with a step of 2deg/min. The voltage was set at 40KV and the current set at 30mA.

RESULTS AND DISCUSSION

1. Calorimetric investigation

Figure 1 shows DSC curves of as-quenched samples of amorphous $Fe_{78}Tm_2B_{20}$ and $Fe_{76}Tm_4B_{20}$ alloys at 20^0C/min heating rate of crystallization, respectively. As in Fig.1(a) the DSC curve of amorphous $Fe_{78}Tm_2B_{20}$ shows a sharp exothermic peak with maximum at 545^0C and some broad and small exothermic peaks at high temperatures. The sharp peak at 545^0C indicates the first phase of crystallization. This means that a single crystalline phase like α - Fe may grow in the amorphous matrix[ref]. The broad and small exothermic peaks at high temperature region(800^0C - 1000^0C) may indicate the growth of other crystalline phases in the material.

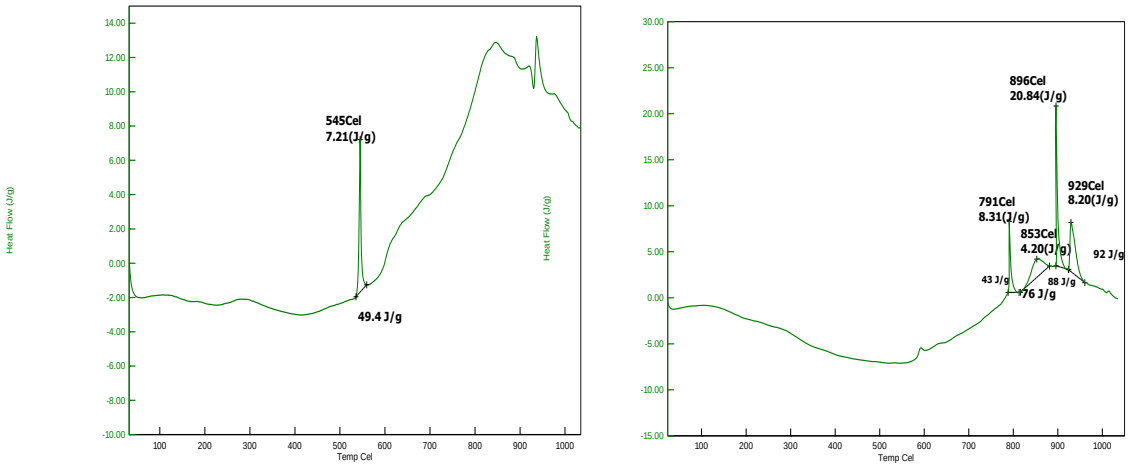

(a) **(b)**

Figure 1: DSC curves of amorphous $Fe_{78}Tm_2B_{20}$ and $Fe_{78}Tm_4B_{20}$ alloys at 20 ^{0}C /min

As in Fig.1(b), the DSC curve of amorphous $Fe_{76}Tm_4B_{20}$ shows a sharp exothermic peak with maximum at 896^0C around which two small exothermic peaks and some broad peak are observed at high temperatures(800^0C - 1000^0C). These are at 791^0C, 929^0C and 853^0C, respectively. The sharp peak at 896^0C indicates another phase of crystallization. Thus Fig. 1(b) shows growth of multi phases in the crystallized sample. The peaks observed in Fig.1(b) also got reflected in Fig.1(a). The broad and sharp exothermic peaks indicate the growth of other crystalline phases in the material. However, in such a large temperature range, important structural transformations may occur in the alloy, as it evolves from a metastable amorphous state to a stable crystalline one. Thus, Fig. 1(b) shows the multi stage crystallization with the growth of different phases in the crystallization process. This confirms that as the concentration of Tm increases in Fe-B, the crystallization process changes.

2. XRD measurements

Figures 2(a) and 2(b) show the room temperature XRD patterns for the samples of amorphous $Fe_{78}Tm_2B_{20}$ and $Fe_{76}Tm_4B_{20}$ alloys for the as-cast and annealed samples at 500°C, 600°C and 700°C for one hour, respectively. The XRD patterns of both the as - cast samples show no prominent peaks indicating that the fresh samples are amorphous.

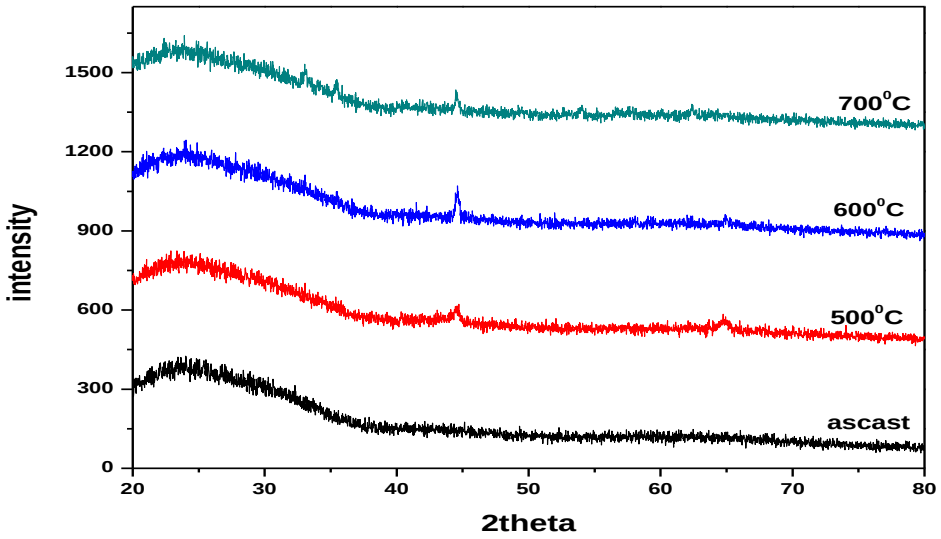

Figure 2(a) Room temperature XRD patterns for the samples of $Fe_{78}Tm_2B_{20}$ alloy for the as-cast and annealed at 500°C, 600°C and 700°C for one hour

As in Fig.2(a), the room temperature XRD of $Fe_{78}Tm_2B_{20}$ annealed at 500°C for one hour shows two small peaks at 2θ values of around 45^0 and 65^0, respectively. The first may arise due to the presence of the crystalline phase α – Fe in the amorphous matrix. The presence of this peak continues in the other annealed temperatures of the sample confirming the existence of the standard phase. The second peak observed at 500°C is not clearly observed in XRD pattern of the sample annealed at 600°C and 700°C for one hour. This means that the second peak which may represent a crystalline phase may get comsumed in the sample at 600°C and 700°C .

As in Fig.2(b), the room temperature XRD of $Fe_{76}Tm_4B_{20}$ annealed at 500°C for one hour shows one small peak at 2θ values of around 43^0. For the sample annealed at 600 °C for one hour, the room temperature XRD showed two peaks around the 2θ values of 45^0 and 67^0. The first may arise due to the presence of the crystalline phase α – Fe in the amorphous matrix. The presence of this peak continues in the other annealed temperatures of the sample confirming the existence of the standard phase. The second peak at 600°C is not clearly observed in XRD patterns of the sample

annealed at 700°C for one hour. This means that the second peak which may represent a crystalline phase may get comsumed at other annealed temperature. Thus, XRD results showed the presence of α – Fe in both the samples.

Table 1 shows the grain size of the crystallized $Fe_{78}Tm_2B_{20}$ and $Fe_{76}Tm_4B_{20}$ alloys calculated using Debye Schurer equation. As in Table 1, the grain size of the samples increases with increase in annealing temperature and with the increase in concentration of Tm in Fe-B.

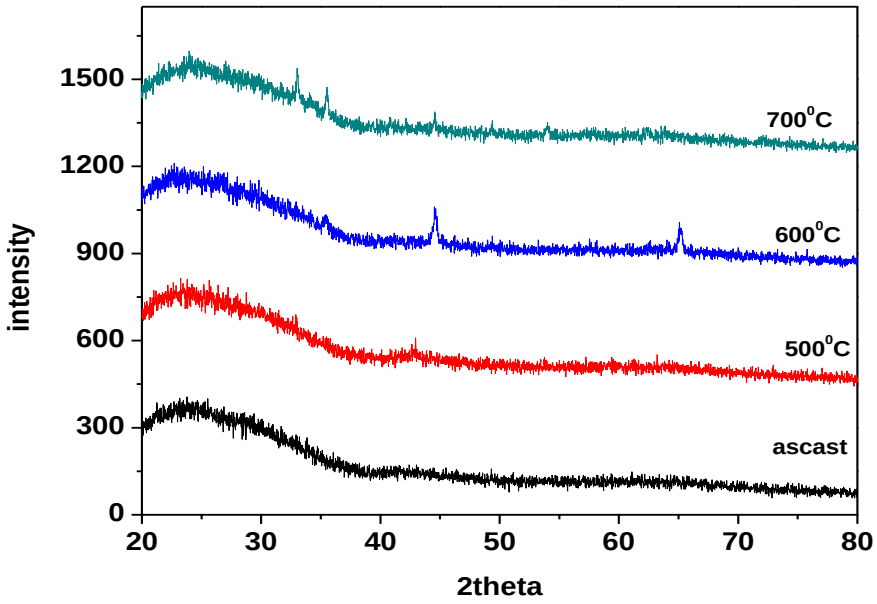

Figure 2(b) Room temperature XRD patterns for the samples of $Fe_{76}Tm_4B_{20}$ alloy for the as-cast and annealed at 500°C, 600°C and 700°C for one hour

Table 1

Annealing Temperatures (^{0}C)	$Fe_{78}Tm_2B_{20}$ (nm)	$Fe_{76}Tm_4B_{20}$ (nm)
500	0.20	----
600	0.27	0.29
700	0.30	0.36

The grain size of crystallized $Fe_{78}Tm_2B_{20}$ and $Fe_{76}Tm_4B_{20}$ alloys calculated using Debye Schurer equation

3. Crystallization Kinetics

According to Kissinger's method [5,6], the transformation under non-isothermal condition is represented by a first-order reaction. More over, the concept of nucleation and growth has not been included in Kissinger equation.

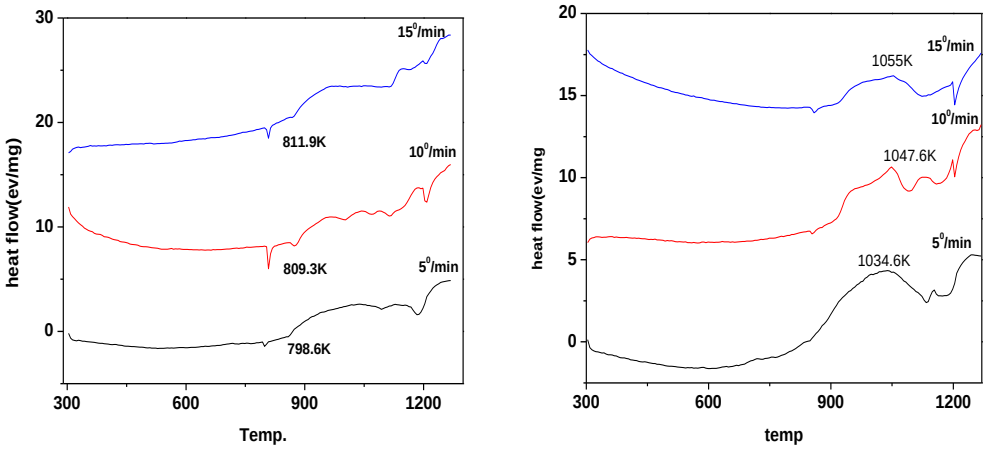

Figure 3: DSC curves of amorphous $Fe_{78}Tm_2B_{20}$ and $Fe_{76}Tm_4B_{20}$ alloys at heating rates 5 ^{0}K/min, 10 ^{0}K/min, and 15 ^{0}K/min

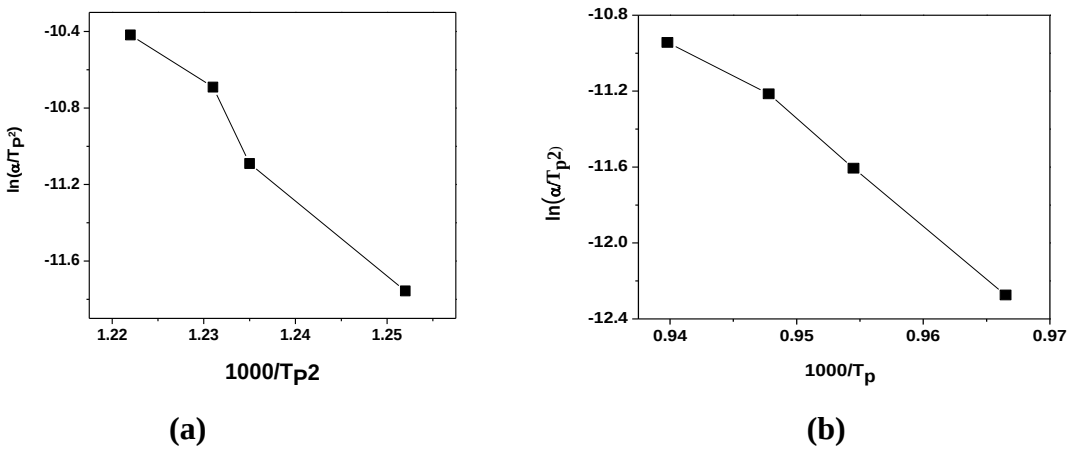

Figure 4: ln (α /T_p^2) vs. (1000/ T_p) of amorphous $Fe_{78}Tm_2B_{20}$ and $Fe_{76}Tm_4B_{20}$ alloys plotted using Kissinger Method

Matusita et al.[7] have developed a method on the basis of the fact that crystallization does not advance by an n^{th} order reaction but by a nucleation and growth process. They emphasized that crystallization mechanism such as bulk crystallization or surface crystallization should be taken into account for obtaining activation energy. Augis and Bennett method [8] is helpful in obtaining kinetic parameters such as frequency factor (*k_0)* along with activation energy (E_a) of crystallization and therefore preferred for the calculation of the kinetics over the other models [9]. Figure 3 shows DSC curves of amorphous $Fe_{78}Tm_2B_{20}$ and $Fe_{76}Tm_4B_{20}$ alloys at the heating rates of 5 ^{0}K/min, 10 ^{0}K/min and 15 ^{0}K/min, respectively. From Fig. 3, one can observe that the increase in the heating rate shifts the peak position to higher temperatures.

The activation energy for crystallization of an amorphous alloy under a linear heating rate can be estimated using Kissinger's peak shift method, which relates the peak temperature, T_p, with heating rate (α) through the equation

$$\ln (\alpha/T_p^2) = -(E_a/RT_p) + \ln(k_0R/E_a) \text{----------(1)}$$

where E_a is the activation energy for crystallization, k_0 the frequency factor which is defined as the number of attempts made by the nuclei per second to overcome the energy barrier and and R is the universal gas constant. This also provides information for the calculation of number of nucleation sites, present in the material for crystal growth [5]. Figure 4 shows the graphs of $\ln (\alpha /T_p^2)$ vs $1000/T_p$ of amorphous $Fe_{78}Tm_2B_{20}$ and $Fe_{76}Tm_4B_{20}$ alloys. The activation energy(E_a) and the frequency factor (k_0) for crystallization peak calculated using Kissinger's peak shift method for the given samples are given in Table 2.

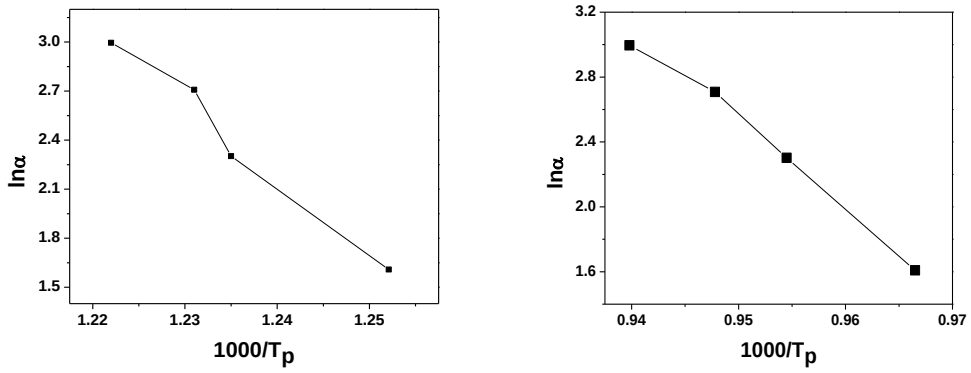

(a) **(b)**

Figure 5: ln (α) vs. (1000/ T_p) of amorphous $Fe_{78}Tm_2B_{20}$ and $Fe_{76}Tm_4B_{20}$ alloys plotted using Matusita-Sakka Method.

The activation energy for crystallization of an amorphous alloy under a linear heating rate can also be estimated using Matusita-Sakka's peak shift method, which relates the peak temperature, T_p, with heating rate (α) through the equation

$$\ln(\alpha) = -(E_a/RT_p) + \text{constant} \text{----------} (2)$$

where E_a is the activation energy for crystallization and R is the universal gas constant. Figure 5 shows the

graph s of ln (α) vs $1000/T_p$ of amorphous $Fe_{78}Tm_2B_{20}$ and $Fe_{76}Tm_4B_{20}$ alloys . The activation energy calculated using Matusita-Sakka's peak shift method for the given samples, is given in Table 2.

Table 2: Composition, Activation Energy, E_a (kJouls/mole) and Frequency factor, k_o $(sec)^{-1}$ of amorphous $Fe_{78}Tm_2B_{20}$ and $Fe_{76}Tm_4B_{20}$ alloys

COMPOSITION	Activation Energy, E_a (kJouls/mole)				Frequency factor, k_o $(sec)^{-1}$	
	Kessinger's Method	Augis-Bennet's Method	Matusita-Sakka's Method	Average (kJouls/mole)	Kessinger's Method	Augis-Bennet's Method
$Fe_{78}Tm_2B_{20}$	379.8	384.43	391.67	385.30	$2.47x10^{21}$	$8.6\ 7x10^{22}$
$Fe_{76}Tm_4B_{20}$	422.7	429.83	440.06	430.86	$5.39x10^{17}$	$2.51x10^{19}$

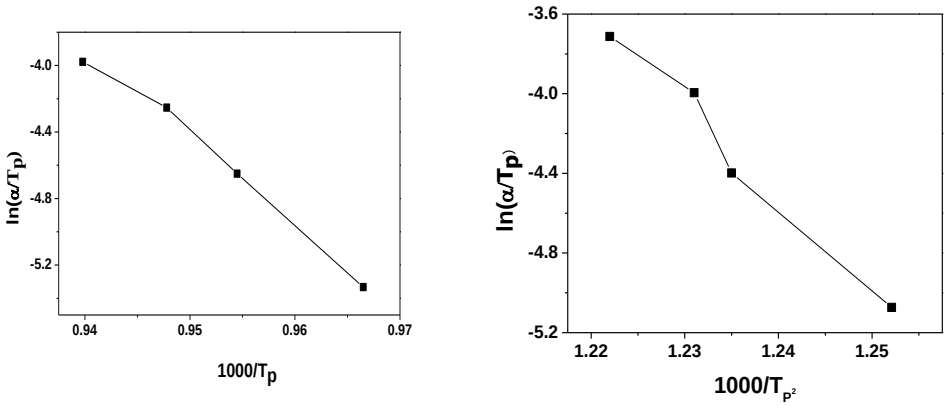

(a) **(b)**

Figure 6: ln (α) vs. ($1000/T_p$) of amorphous $Fe_{78}Tm_2B_{20}$ and $Fe_{76}Tm_4B_{20}$ alloys plotted using Augiss and Bennet Method

The activation energy for crystallization of an amorphous alloy under a linear heating rate can be estimated using Augis & Bennett method, which relates the peak temperature, T_p, with heating rate (α) through the equation

$$\ln(\alpha/T_p) = -E_a / RT_p + \ln k_o \text{ ----------(3)}$$

where E_a is the activation energy for crystallization, R is universal gas constant and k_0 the frequency factor. Figure 6 shows the graph of $\ln(\alpha/T_p)$ vs. $1000/T_p$ of amorphous $Fe_{78}Tm_2B_{20}$ and $Fe_{76}Tm_4B_{20}$ alloys. The activation energy (E_a)and the frequency factor (k_0) for crystallization peak using Augis & Bennett method for the given samples are also given in Table 2.

Table 2 also gives the average value of activation energy of the samples. Thus, the average activation energy for primary crystallization of amorphous $Fe_{78}Tm_2B_{20}$ and $Fe_{76}Tm_4B_{20}$ alloys using the above three methods is determined as 385.30kJouls/mole and 430.86 kJouls/mole, respectively. It is also observed that activation energies of amorphous alloys calculated by means of the different theoretical models differ slightly from each other. This difference in the activation energy as calculated with the different models may be attributed to the different approximations used in the models. Similarly, the frequency factor k_o of amorphous $Fe_{78}Tm_2B_{20}$ and $Fe_{76}Tm_4B_{20}$ alloys using Kissinger method is found to be $2.47x10^{21}$ $(sec)^{-1}$ and $5.39x10^{17}$ $(sec)^{-1}$, respectively. Also, the frequency factor k_o of amorphous $Fe_{78}Tm_2B_{20}$ and $Fe_{76}Tm_4B_{20}$ alloys using Augis-Bennet's method is found to be $8.6\ 7x10^{22}$ $(sec)^{-1}$ and $2.51x10^{19}$ $(sec)^{-1}$, respectively.

CONCLUSIONS

The crystallization process of amorphous $Fe_{76}Tm_4B_{20}$ alloy strongly differs from that of amorphous $Fe_{78}Tm_2B_{20}$ alloy. The grain size of the samples increases with increase in annealing temperature and with the increase in concentration of Tm in Fe-B. XRD results showed the presence of α – Fe.

The average activation energy for primary crystallization of amorphous $Fe_{78}Tm_2B_{20}$ and $Fe_{76}Tm_4B_{20}$ alloys using the above three methods is found to be 385.30kJouls/mole and 430.86 kJouls/mole, respectively. The slight difference in the activation energy calculated using different models may be attributed to the different approximations used in these models. The frequency factor of amorphous $Fe_{78}Tm_2B_{20}$ and $Fe_{76}Tm_4B_{20}$ alloys using Kissinger method is found to be $2.47x10^{21}$ $(sec)^{-1}$ and $5.39x10^{17}$ $(sec)^{-1}$, respectively. The frequency factor of amorphous $Fe_{78}Tm_2B_{20}$ and $Fe_{76}Tm_4B_{20}$ alloys using Augis-Bennet's method is found to be $8.6\ 7x10^{22}$ $(sec)^{-1}$ and $2.51x10^{19}$ $(sec)^{-1}$, respectively.

ACKNOWLEDGEMENTS

The authors M.D.V. Srilalitha and B. Bhanu Prasad acknowledge the encouragement given by the management, the Principal, HOD of Sciences & Humanities and the staff of M.V.S.R. Engineering College, Nadergul, Hyderabad.

REFERENCES

[1] Hansen P Handbook of Magnetic Materials Vol 6, ed K.H.J. Buschow(Amsterdam: North Holland-Elsevier) pp 289-452

[1] Carter, C.B. & Norton, M.G. (2007), Ceramic Materials Science and Engineering, Springer, ISBN-10: 0387462708, New York, USA.

[2] Araújo, E.B. & Idalgo, E. *Journal of Thermal Analysis and Calorimetry*, **95** (2009) 37

[3] Araujo, E.B., Idalgo, E., Moraes, A.P.A., Souza Filho, A.G. & Mendes Filho, J., *Materials Research Bulletin*, **44** (2009) 1596

[4] Kissinger, H.E., *AnaliticalChemistry*, **29**, (1957) 1702.

[5] Kissinger, H.E., *Journal of Research of the National Bureau of Standards*, **57** (1956) 217

[6] Matusita, K. & Sakka, S. *Bulletin of the Institute for Chemical Research*, **59** (1981) 159

[7] Augis, A.J. & Bennett, J.E., *Journal of Thermal Analysis and Calorimetry*, **13** (1978) 283

[8] Deepika, Jain, P.K., Rathore, K.S. & Saxena, N.S. *Journal of Non-Crystalline Solids*, **355** (2009) 1274